Chapter 4

Semiclassical periodic orbit quantization

4.1 The Van Vleck propagator

The Van Vleck formula is a semiclassical approximation for the usual propagator in quantum mechanics

$$G(x',t';x,t) \equiv < x'|U(t',t)|x > \Theta(t) \tag{4.1}$$

where $U(t',t)$ is the unitary time evolution operator for some quantum system which might be time dependant, and $\Theta(t)$ is the unit step- or Heaviside function. The Van Vleck formula is the starting point for a number of derivations, approximations and intuitive leaps which take one from exact quantum expressions to a variety of results expressing energy eigenvalues and their correlations, wave functions and matrix elements in terms of classical periodic orbits.

The propagator

$$G(x',t';x,t) \equiv < x',t'|e^{\frac{i}{\hbar}\hat{H}(t'-t)}|x,t > \tag{4.2}$$

fulfills

$$(\hat{H} - i\hbar\frac{\partial}{\partial t})G(x',t';x,t) = -i\hbar\delta(t-t'). \tag{4.3}$$

To derive the semiclassical approximation to the propagator one can take as the starting point the solution to the initial value problem of quantum mechanics following the WKB procedure. This can be done since the propagator can be considered as the solution $G(x',t';x,t)$ of the time-dependant Schrödinger equation, subject to the initial condition $G(x',t';x,t) = \delta(x-x')$ at $t=0$. To solve the initial value problem in the WKB approximation we start by making the following ansatz. Suppose we are given an initial wave function of the form

$$\psi(x,t) = A_0(x)\exp[iS_0(x)/\hbar], \tag{4.4}$$

where the initial amplitude $A_0(x)$ is assumed to be real and positive, and $S_0(x)$ is the initial action. We can then make the assumption that the wave function at a later time can again be expressed in the same WKB form i.e.

$$\psi(x,t') \quad = \quad A(x,t')\exp[iS(x,t')/\hbar]. \tag{4.5}$$

Our problem is to find the final amplitude $A(x,t')$ and action $S(x,t')$. Inserting (4.4) into the Schrödinger equation, expanding in powers of $\hbar$, and neglecting terms of order $\hbar$ and higher we get to the lowest order

$$H(x,\frac{\partial S(x,t')}{\partial x};t') + \frac{\partial S(x,t')}{\partial t'} \quad = \quad 0 \tag{4.6}$$

which we recognize as the time dependant Hamilton-Jacobi equation for the action S. Here the momentum dependance has been replaced by $p = \partial S/\partial x$. This result can easily be obtained for standard Hamiltonians of the form $H(x,p,t) = p^2/2m + V(x,t)$, but is actually valid for any Hamiltonian which has a classical limit. The result of the expansion to the first order in $\hbar$ is the so called amplitude transport equation which can be conveniently expressed in terms of the density ρ, defined by

$$\rho(x,t) \quad \equiv \quad |A(x,t)|^2. \tag{4.7}$$

Since ρ can be interpreted as the probability density it can be thought of as a configuration space density of *classical* particles. The amplitude transport equation then takes the shape of the usual continuity equation known from fluid mechanics and electrodynamics

$$\frac{\partial \rho(x,t)}{\partial t} + \frac{\partial}{\partial x}\left[\rho(x,t)v(x,t)\right] \quad = \quad 0, \tag{4.8}$$

where the x derivative is a divergence in more than one dimension, and where we have defined the velocity field

$$v(x,t) \quad \equiv \quad \frac{1}{m}\frac{\partial H(x,p;t)}{\partial p} \tag{4.9}$$

with $p = \partial S(x,t)/\partial x$. In the following we shall assume that $m = 1$. As we see the continuity equation is driven by the solution S of the autonomous Hamilton-Jacobi equation, and it is therefore necessary to first solve this for S. We will not solve the equations here but merely state the results. A very good derivation of the solution can be found in [40]. The solution to the Hamilton-Jacobi equation is given by

$$S(x',t') \quad = \quad S(x,t) + R(x',t';x,t) \tag{4.10}$$

where $R(x',t';x,t)$ is the line integral $\int(pdx - Hdt)$ along a classical orbit connecting (x,t) with (x',t').

The solution of the continuity equation can be obtained in a straightforward manner by applying probability conservation. Because of the interpretation of ρ being a classical density of particles, conservation of the number of particles allows us to write

$$\rho(x',t')dx' \quad = \quad \rho(x,t)dx, \tag{4.11}$$

or, in terms of the amplitudes,

$$A(x',t') = A(x,t)|\det\frac{\partial x}{\partial x'}|^{1/2}, \tag{4.12}$$

where the determinant determines the volume ratio of an evolved configuration space volume element to the initial volume element. The solution to the initial value problem in WKB theory therefore takes the form

$$\psi(x',t') = A(x,t)|\det\frac{\partial x}{\partial x'}|^{1/2}\exp(\frac{i}{\hbar}[S(x,t)+R(x',t';x,t)]) \tag{4.13}$$

for the case where the initial action function develops no singularities in the elapsed time. In the case where the action function goes through *caustics* one has to deal with several branches of the action function and the solution to the initial value problem correspondingly changes to be a sum over WKB terms like (4.13) - one for each branch

$$\psi(x',t') = \sum_b A_b(x,t)|\det\frac{\partial x}{\partial x'}|^{1/2}\exp(\frac{i}{\hbar}[S(x,t)+R_b(x',t';x,t)-i\kappa\frac{\pi}{2}]) \tag{4.14}$$

where κ is the integer *Maslov index* absorbing the possible change of sign of the amplitude [40]

To get the semiclassical expression of the propagator we therefore just have to put in the initial value of the propagator in the WKB form. This however is not directly possible since we have $G(x,x',0) = \delta(x-x')$ which cannot be realized in the WKB ansatz (4.4). However, by working in momentum space the initial wave function becomes completely well defined, and we can carry out the very same calculations for this wave function. After evolving the momentum wave function in time t we can then transform the solution back (by a stationary phase approximation) to configuration space and thereby finally obtain an expression for the propagator. The result of this procedure yields

$$\begin{aligned} G(x',t';x,t) &= \frac{1}{(2\pi i\hbar)^{f/2}}\sum_b|\frac{\partial p_b}{\partial x'}|^{1/2} \\ &\times \exp[\frac{i}{\hbar}R_b(x',t';x,t)-i\kappa_b\frac{\pi}{2}], \end{aligned} \tag{4.15}$$

where $p_b = p_b(x',t,t')$ is the initial momentum of the particle ending up at the p'th branch (x',p'_b) at time t' and where $i^{f/2}$ means $e^{if\pi/4}$. This is finally the Van Vleck expression of the propagator. We note that all orbits connecting x to x' in time t carry their own amplitude contributions, and that these can interfere since they are added as complex numbers.

Next we can relate the propagator to the density of states. If we start out with the special case when $\hat{H}$ is independant of time, then the propagator only depends on $t'-t$ so we can set $t=0$ and just write $G(x,x';t)$. In that case we have

$$G(x,x';t) = \Theta(t)\sum_n e^{-iE_nt/\hbar}|n><n| \tag{4.16}$$

where the sum is over the (assumed discrete) set of energy eigenstates. Next we can define the energy dependant Greens function

$$G(x,x';E) \equiv \frac{1}{i\hbar}\int_{-\infty}^{\infty} dt\, e^{iEt/\hbar} G(x,x';t) \tag{4.17}$$

Since $G(t) = 0$ for $t < 0$ the lower limit can be replaced by 0. Here E is a complex energy like variable. The integral is guaranteed to converge only for $\mathrm{Im}E > 0$, where it defines an analytic function $\tilde{G}(E)$. $\tilde{G}(E)$ is then defined for $\mathrm{Im}E \geq 0$ by analytic continuation. Inserting (4.16) into (4.17) gives

$$\begin{aligned} \tilde{G}(E) &= \sum_n \frac{|n><n|}{E-E_n} \\ &= \frac{\mathbf{1}}{E-E_n} \end{aligned} \tag{4.18}$$

the resolvant operator. Finally we define $g(E)$ as the trace of $\tilde{G}(E)$,

$$\begin{aligned} g(E) &\equiv \mathrm{Tr}\,\tilde{G}(E) \\ &= \sum_n \frac{1}{E-E_n} \end{aligned} \tag{4.19}$$

which has poles at the energy eigenvalues. If we now replace the complex E by $E + i\epsilon$, where now E is real and $\epsilon > 0$, we note that

$$\begin{aligned} \mathrm{Im}\left(\frac{1}{E+i\epsilon-E_n}\right) &= \frac{-\epsilon}{(E-E_n)^2+\epsilon^2} \\ &\to -\pi\delta(E-E_n) \quad \text{for } \epsilon \to 0. \end{aligned} \tag{4.20}$$

Therefore we have

$$\lim_{\epsilon\to 0}\frac{-1}{\pi}\mathrm{Im}g(E+i\epsilon) = \sum_n \delta(E-E_n) \equiv n(E)$$

where $n(E)$ is the density of states.

To proceed, we can obtain a semiclassical expression for the density of states by inserting the Van Vleck propagator into the exact quantum mechanical expression for the density of states. This calculation is not done here - we will only state the most important steps. A very good derivation of all the necessary steps is done in the lecture notes of Littlejohn [40].

First, when making the Fourier transform to get $G(x,x';E)$ we make a saddlepoint approximation which provides us with a simple semiclassical expression for the energy domain propagator. We then find that the orbits that before were parametrized by time now can be parametrized by the energy E according to the stationary phase condition used in the saddle point approximation of the Fourier transform. Second, by taking the trace we have to consider only the orbits that are closed in configuration space. By also evaluating the trace by stationary phase approximation we obtain that the orbits should also be closed in momentum space, so that we end up considering the *periodic orbits* of the

system. The trace integral is then divided up into two parts: one integral along the periodic orbit which basically yields the *cycle period* of the periodic orbit, and $f-1$ integrals in orthogonal directions to the cycle, which are evaluated then by stationary phase approximation. Then finally one has to work on the final expression to relate the transverse stability properties of the periodic orbit to the result of the transverse Gaussian integrations. The result for the trace is

$$\mathrm{tr}G(E) = \overline{g}(E) + \frac{1}{i\hbar}\sum_p T_p \sum_r^{\infty} \frac{e^{-\frac{i}{\hbar}S_p(E)r + i\pi\frac{\kappa_p}{2}r}}{|\det\left(\mathbf{1}-\mathbf{J}_p^r\right)|^{\frac{1}{2}}}\ , \tag{4.21}$$

whereas the result for the density of states then finally reads

$$n(E) \;=\; \frac{1}{\pi\hbar}\sum_p T_p \sum_{r=1}^{\infty} \frac{\cos r(S_p(E)/\hbar - \kappa_p\pi/2)}{|\det(\mathbf{1}-\mathbf{J}_p^r)|^{1/2}} \tag{4.22}$$

where the sum is over the *prime* periodic orbits, $\mathbf{J}_p$ is the Jacobian containing the transverse stabilities of the surface of section or Poincare mapping and κ_p is the Maslov index associated with the orbit. A prime periodic orbit is just one single representative of the periodic manifold and all the other periodic orbits lying on top of this can be obtained by a time shift and r traversals of the orbit, where r counts the number of repetitions. Also in the formula (4.22) we have neglected the contribution from zero length orbits which gives the "averaged density of states" $\bar{n}(E)$. This is given by the Thomas-Fermi (or the first Weyl) term

$$\bar{n}(E) \;=\; \int \frac{d^f q d^f p}{(2\pi\hbar)^f}\delta(H(q,p)-E) \tag{4.23}$$

The formula (4.22) is known as the Gutzwiller trace formula, first derived by Gutzwiller [35] in 1971. Gutzwiller took as the starting point for his derivation the path integral expression for the trace of the propagator, and did not use the Van Vleck propagator directly. We find the derivation sketched above more in the spirit of modern analysis of dynamical systems in terms of periodic orbits.

4.2 The Gutzwiller-Voros zeta function

The problem with the Gutzwiller trace formula is that it diverges precisely where one would like to use it. Crude estimates of its radius of convergence lead to the observation that the entire physical spectrum may be out of reach. The problem is cured by going from the trace formula to the related spectral determinant, which can be formally written

$$\Delta(E) \;\equiv\; \prod_n (E-E_n), \tag{4.24}$$

which is related to the trace by

$$\mathrm{Tr}G(E) \;=\; \frac{d}{dE}\ln\Delta(E), \tag{4.25}$$

and which has zeros at the eigenenergies. A semiclassical expression for the spectral determinant was first obtained by Voros [56] using the results of Gutzwiller. The analog of (4.25) in the semiclassical case can be derived easily for the 2-dimensional case of unstable periodic orbits by looking at the oscillatory part of the Gutzwiller trace formula. In that case the determinant in the denominator takes the form

$$\det(\mathbf{1}-\mathbf{J}_p^r) \;=\; (1-\Lambda_p^r)(1-\Lambda_p^{-r}) \tag{4.26}$$

because of the symplectic structure of the Jacobian. For the oscillatory part of the density of states we then have

$$\begin{aligned}
n(E) &= \mathrm{Re}\;\frac{1}{\pi\hbar}\sum_p\sum_{r=1}^{\infty}T_p\frac{e^{i(S_p(E)/\hbar-\kappa_p\pi/2)r}}{|\Lambda_p|^{r/2}(1-\Lambda_p^{-r})}\\
&= \mathrm{Re}\;\frac{1}{\pi\hbar}\sum_p\sum_{r=1}^{\infty}\sum_{j=0}^{\infty}T_p\left(|\Lambda_p|^{-1/2}\Lambda_p^{-j}e^{i(S_p(E)/\hbar-\kappa_p\pi/2)}\right)^r\\
&= \mathrm{Re}\;\frac{1}{\pi\hbar}\sum_p\sum_{j=0}^{\infty}T_p\frac{|\Lambda_p|^{-1/2}\Lambda_p^{-j}e^{i(S_p(E)/\hbar-\kappa_p\pi/2)}}{1-|\Lambda_p|^{-1/2}\Lambda_p^{-j}e^{i(S_p(E)/\hbar-\kappa_p\pi/2)}}\\
&= -\frac{1}{\pi}\mathrm{Im}\sum_p\sum_{j=0}^{\infty}\frac{\partial}{\partial E}\ln\left(1-|\Lambda_p|^{-1/2}\Lambda_p^{-j}e^{i(S_p(E)/\hbar-\kappa_p\pi/2)}\right)\\
&= -\frac{1}{\pi}\mathrm{Im}\frac{\partial}{\partial E}\ln Z(E)
\end{aligned} \tag{4.27}$$

where $Z(E)$ is a dynamical zeta function like expression for the semiclassical spectral determinant. In the following we shall denote this determinant the *Gutzwiller-Voros* determinant or the Gutzwiller-Voros zeta function when referring to this. We see that the Gutzwiller-Voros determinant has the structure

$$\begin{aligned}
Z(E) &= \prod_{j=0}^{\infty}\zeta_j^{-1}(E)\\
&= \exp\left(-\sum_p\sum_{r=1}^{\infty}\frac{e^{iS_p(E)r/\hbar-\kappa_p\pi/2}}{r\sqrt{|\Lambda_p|^r}(1-\Lambda_p^{-r})}\right),
\end{aligned} \tag{4.28}$$

where

$$\zeta_j^{-1}(E) \;=\; \prod_p(1-t_p/\Lambda_p^j(E)), \tag{4.29}$$

and we have defined the j'th weight associated with the p'th cycle as

$$t_p(E) \;=\; z^{n_p}\frac{e^{iS_p(E)/\hbar-\kappa_p\pi/2}}{|\Lambda_p|^{1/2}}. \tag{4.30}$$

where z is a book-keeping variable that keeps track of the topological cycle length n_p, used to expand zeta functions and determinants (see sect. 3.2).

An infinite product over prime periodic orbits like the one in (4.29) is denoted a dynamical zeta function [45] by analogy to the *Riemann zeta function*

which is an infinite product over the prime integers

$$\begin{aligned} \zeta_R^{-1}(s) &= \left(\sum_{n=1}^{\infty} n^{-s}\right)^{-1} \\ &= \prod_p (1 - e^{-s \ln p}). \end{aligned} \tag{4.31}$$

As in many applications the wave number k is a more natural choice of variable than the energy E, we shall henceforth replace E by k in all semi-classical formulas.

The Gutzwiller trace formula, apart from the quantum and Maslov phases, differs from the classical trace formula in two aspects. One is the volume term $\overline{g}(E)$ in (4.21) which is a missing from our version of the classical trace formula. While an overall pre-factor does not affect the location of zeros of the determinants, it might play a role in relations such as functional equations for zeta functions. The other difference is that the quantum kernel leads to a square root of the cycle Jacobian determinant, a reflection of the relation probability = (amplitude)^2. The $1/\sqrt{\det(1 - \mathbf{J}_p)}$ weight leads in turn to the product representation

$$Z(k) = \prod_p \prod_{k=0}^{\infty} \left(1 - t_p/\Lambda_p^k\right) \ , \tag{4.32}$$

which differs from the classical Fredholm determinant (3.12) by missing exponent $k + 1$.

Chapter 5

Convergence

5.1 Entire spectral determinants in semiclassics

Even though the divergence problem with the Gutzwiller trace formula could be partially solved by considering spectral determinants instead of trace formulas, the divergence problem is not cured in a satisfying way. This is due to the fact that the Gutzwiller-Voros zeta function has a finite radius of convergence (seen as parallel stribes), and if we look for scattering resonances in the complex k-plane we will encounter this [14] when searching for nonleading zeros. It is therefore important to get a spectral determinant which has a larger domain of analyticity or which might even be entire. As we saw in section 3.1 Such spectral- or Fredholm determinants are known in the case of maps and in the case of classical flows.

In this section we start by taking a look at the first attempts to improve the analytic properties of semiclassical spectral determinants (the Gutzwiller-Voros spectral determinant), by studying the so-called quantum Fredholm determinant introduced by Cvitanović and Rosenqvist [13]. Next we follow the work by Vattay who introduced a multiplicative operator which is capable of evolving *quasi-classical* wavefunctions and which has an *entire* related spectral determinant. Finally we derive the general N-dimensional formula of this entire determinant.

5.1.1 The quantum Fredholm determinant

While various periodic orbit formulas may be formally equivalent, in practice some are vastly preferable to others. Trace formulas, such as the thermodynamic averages in classical dynamics, and the semi-classical Gutzwiller trace formula in quantum mechanics are difficult to use for anything other than the leading eigenvalue estimates. The convergence of cycle expansions of zeta functions and Fredholm determinants depends on their analytic properties; and as we saw in section 3.1 the classical Fredholm determinants are entire functions[48]. A

formal analogy to the classical case leads us to the introduction of the *quantum Fredholm determinant* [13], which for two-dimensinal Hamiltonian flows reads

$$\begin{aligned} F_{qm}(E) &= \prod_p \prod_{k=0}^{\infty} \left(1 - \frac{e^{-\frac{i}{\hbar}S_p(E)+i\pi m_p/2}}{|\Lambda_p|^{1/2}\Lambda_p^k}\right)^{k+1} \\ &= \exp\left(-\sum_p \sum_{r=1}^{\infty} \frac{e^{iS_p(E)r/\hbar-\kappa_p\pi/2}}{r\sqrt{|\Lambda_p|^r}(1-\Lambda_p^{-r})^2}\right), \end{aligned} \tag{5.1}$$

as an alternative to the Gutzwiller-Voros zeta function

$$Z(E) = \prod_p \prod_{k=0}^{\infty} \left(1 - \frac{e^{-\frac{i}{\hbar}S_p(E)+i\pi m_p/2}}{|\Lambda_p|^{1/2}\Lambda_p^k}\right). \tag{5.2}$$

We present here the numerical evidence in support of the conjecture of ref. [13]:

For Axiom A systems the quantum Fredholm determinant has a larger domain of analyticity than the Gutzwiller-Voros zeta function.

We shall consider here only the purely hyperbolic flow of the 3-disk repeller

The conjecture we test in this section, asserts that one may replace the Gutzwiller-Voros zeta function (4.32) by the *quantum Fredholm determinant* (5.1), *ie.* the Fredholm determinant (3.12) with the *quantum* weights t_p, without disturbing the leading semi-classical eigenvalues, but improving the convergence of cycle expansions used in evaluating the spectrum.

The form of the quantum weight (4.30) suggests that the quantum evolution operator should be approximated by a classical evolution operator with a quantum weight:

$$\mathcal{L}^t(y,x) = \delta(y - f^t(x))\sqrt{|\Lambda^t(x)|}e^{-\frac{i}{\hbar}S^t(x)+i\pi m_p(x)/2} .$$

However, even though the Jacobians are multiplicative i.e. $\mathbf{J}_{ab} = \mathbf{J}_a \cdot \mathbf{J}_b$, the same rule does not apply to their eigenvalues so in general we have $\Lambda_{ab} \neq \Lambda_a\Lambda_b$, and the above operator is therefore not multiplicative along the trajectory, and consequently does not satisfy the assumptions required by the theorems that guarantee that a Fredholm determinant is entire [47]. Nevertheless, our numerical results support the conjecture that the $|\Lambda|^{1/2}$ weighted determinant has a larger domain of analyticity than the commonly used Gutzwiller-Voros zeta function and that some related determinant (see section 5.2)might even be entire.

5.1.2 Abscissa of absolute convergence

Consider the approximation (3.4) in the case of the Gutzwiller trace formula (4.21):

$$\mathrm{Tr}\, G(k) \approx \sum_p T_p \sum_r^{\infty} \frac{e^{-\frac{i}{\hbar}S_p(k)r + i\pi m_p r/2}}{|\Lambda_p^r|^{1/2}} .$$

This approximation omits the non leading $\approx 1/\Lambda_p$ terms that vanish in the $t \to \infty$ limit and do not affect the leading eigenvalues. If the phases conspire to partially cancel contributing terms, the sum diverges for a larger value of $\mathrm{Im}(k)$. The abscissa of absolute convergence in the complex k plane is obtained by maximizing the sum, *ie.* replacing all terms by their absolute values:

$$\mathrm{tr}G(k) \approx \sum_p T_p \sum_r^{\infty} \frac{e^{T_p \mathrm{Im}(k) r}}{|\Lambda_p^r|^{1/2}} .$$

(we have for simplicity taken S_p to be the action for billiards, $S_p/\hbar = T_p k$). The value of $\mathrm{Im}(k)$ for which this sum diverges determines the abscissa of absolute convergence. We can also use determinants to accurately estimate this abscissa of absolute convergence, by replacing all cycle weights t_p in (3.12) by their absolute values.

To evaluate the abscissa of absolute convergence of the Gutzwiller-Voros zeta function we first note that inserting the identity $1 = (1-1/\Lambda_p^r)/(1-1/\Lambda_p^r)$ into the exponent of Gutzwiller-Voros zeta function (4.30), one obtains the following relation between the Gutzwiller-Voros zeta function and the quantum Fredholm determinant:

$$Z(k) = \frac{F_{qm}(k)}{F_{\frac{1}{2}}(k)} ,$$

where

$$F_{\frac{1}{2}}(k) = \exp\left(- \sum_p \sum_{r=1}^{\infty} \frac{1}{r} \frac{t_p^r}{\Lambda_p^r (1 - 1/\Lambda_p^r)^2} \right) . \tag{5.3}$$

The radius of convergence of $Z_{qm}(k)$ is therefore determined by the leading zeros of $F_{\frac{1}{2}}(k)$. To estimate the upper bound on $\mathrm{Im}(k)$ for the zeros of $F_{\frac{1}{2}}$, we omit all signs and phases in the weights in $F_{\frac{1}{2}}$:

$$\hat{F}_{\frac{1}{2}}(k) = \exp\left(- \sum_p \sum_{r=1}^{\infty} \frac{1}{r} \frac{|t_p^r|}{|\Lambda_p^r| (1 - 1/\Lambda_p^r)^2} \right) , \tag{5.4}$$

and compute its leading zero at $\mathrm{Re}(k) = 0$. An example is given in sect. 5.1.3.

5.1.3 Numerical results

In this section we present the evidence that the quantum Fredholm determinant is numerically as convergent as the classical Fredholm determinant, in contrast to the Gutzwiller-Voros zeta function which has a finite radius of convergence.

Following refs. [18, 24, 32, 31], we perform our numerical tests on the 3-disk repeller. The 3-disk repeller is the simplest physical realization of an Axiom A system, particularly convenient for numerical investigations. For billiards the cycle weight t_p required for evaluation of the classical escape rates and correlation spectra is given by (3.12). The action S_p is proportional to the cycle period T_p, and the Maslov index changes by $+2$ for each disk bounce, $\kappa_p = 2n_p$, so the quantum weight (4.30) is given by

$$t_p = (-1)^{n_p} \frac{e^{-ikT_p}}{\sqrt{|\Lambda_p|}} z^{n_p} \,, \tag{5.5}$$

where k = (momentum)$/2\pi$ is the wave-number, and we take velocity = 1, mass = 1.

Cycle expansion (3.19) coefficients $|C_n|$ for different determinants and zeta functions are plotted in figs. 5.1 as function of the topological cycle length n. Zeta functions exhibit exponential falloff, implying a pole in the complex plane, while both the classical and the quantum Fredholm determinants appear to exhibit a faster than exponential falloff, with no indication of a finite radius of convergence within the numerical validity of our cycle expansion truncations.

In particular, the quantum Fredholm determinant enables us to uncover more resonances than what was hitherto accessible by means of the dynamical zeta functions [31, 24, 12]. The eye is conveniently guided to the zeros by means of complex s plane contour plots, with different intervals of the absolute value of the function under investigation assigned different colours; zeros emerge as centers of elliptic neighborhoods of rapidly changing colors (see figs. 5.4). Detailed scans of the whole area of the complex s plane under investigation and searches for the zeros of classical and quantum Fredholm determinants, fig. 5.2, reveal complicated patterns of resonances, with the classical and the semi-classical resonance patterns surprisingly similar. It is known [18] that the leading semi-classical resonances are very accurate approximations to the exact quantum resonances; the semi-classical resonances further down in the s complex plane in fig. 5.2 has first recently been compared with the exact quantum values [63]. This comparison showed that the resonances of the quantum Fredholm determinant though highly convergent, unfortunately did not match the exact data. On the other hand for cycle expansions to order 6 and 7, the Gutzwiller-Voros zeta function gives remarkably good results even in this domain.

Contour plots are also helpful in comparing the domain of convergence of the Fredholm determinant to that of the Gutzwiller-Voros zeta function. As can be seen from fig. 5.4, the quantum Fredholm determinant can be continued

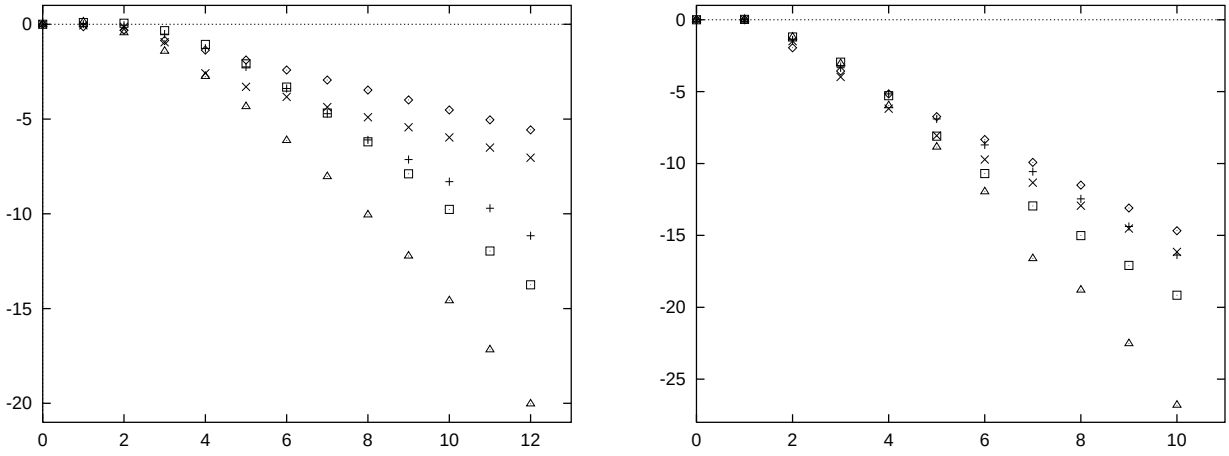

Figure 5.1: (a) $\log_{10}|C_n|$, the contribution of cycles of topological length n to the cycle expansion $\sum C_n z^n$ for 3-disk repeller. Shown are: ($\diamond$) $1/\zeta_0$, ($\times$) the Gutzwiller-Voros zeta function, ($+$) $1/\zeta_0\zeta_1^2$, and ($\Box$) the quantum Fredholm determinant. Exponential falloff implies that $1/\zeta_0$ and the Gutzwiller-Voros zeta function have the same leading pole, canceled in the $1/\zeta_0\zeta_1^2$ product. For comparison, ($\triangle$) the classical Fredholm determinant coefficients are plotted as well; cycle expansions for both Fredholm determinants appear to follow the asymptotic estimate $C_n \approx \Lambda^{-n^{3/2}}$. A_1 symmetric subspace, with center spacing - disk radius ratio $R : a = 3 : 1$, evaluated at the lowest resonance, wave number $k = 7.8727 - 0.3847\,i$, maximal cycle length $n = 8$. (b) Same as (a) , but with $R : a = 6 : 1$. This illustrates possible pitfalls of numerical tests of asymptotics; the quantum Fredholm determinant appears to have the same pole as the quantum $1/\zeta_0\zeta_1^2$, but as we have no estimate on the size of pre-asymptotic oscillations in cycle expansions, it is difficult to draw reliable conclusions from such numerics. See fig. 5.5 for estimate of the quantum Fredholm determinant abscissa of absolute convergence.

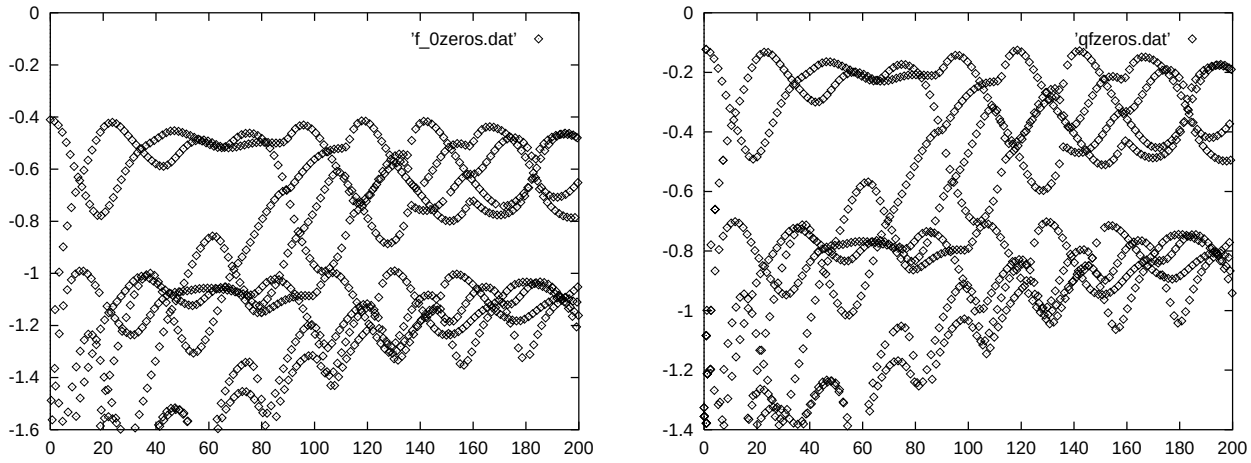

Figure 5.2: Leading resonances in the 3-disk repeller A_1 subspace, (a) for the classical Fredholm determinant, and (b) the 952 leading resonances of the quantum Fredholm determinant F_{qm}. Ratio $R : a = 6 : 0$, cycle expansions truncated at cycle length $n = 8$.

considerably farther down in the complex k plane, in contrast to the dynamical zeta function scans such as those given in ref. [31]. While the zeta functions clearly exhibit a finite radius of convergence, both the classical Fredholm determinant and the quantum Fredholm determinant behave as entire functions. We compute the abscissa of absolute convergence for the Gutzwiller-Voros zeta function by means of (5.4); for the case at hand we obtain the leading zero at $k_{ac} = 0.0 - i\,0.699110157151\ldots$. This estimate might be a bit too crude since the results of Wirzba [63] indicate that to curvature order 7 the Gutzwiller-Voros zeta function gives nice results for the resonances even down to $\mathrm{Im}k = -1.1$, as shown in figure 5.3. Interestingly enough, the apparent border of Gutzwiller-Voros zeta function convergence in fig. 5.4 seems to coincide with $\mathrm{Re}(s) = 0$, $\mathrm{Im}(s) = -1.09653395\ldots$, the zero obtained from $F_{1/2}(k)$ by removing quantum phases, $t_p \to |t_p|$, but keeping the eigenvalue Λ_p sign in (5.3).

5.2 The quasi-classical approximation

In this section we follow Vattay [53] and show how the eigenvalues of the first order partial differential equation derived by the quasi-classical approximation of the Schrödinger equation in the case of an Axiom A flow, can be computed from the trace of a classical operator. The corresponding spectral determinant of the new operator is an entire function in the complex plane in contrast to the usual Gutzwiller-Voros- or quantum Fredholm determinants.

For a single particle of unit mass the Schrödinger equation in a potential U

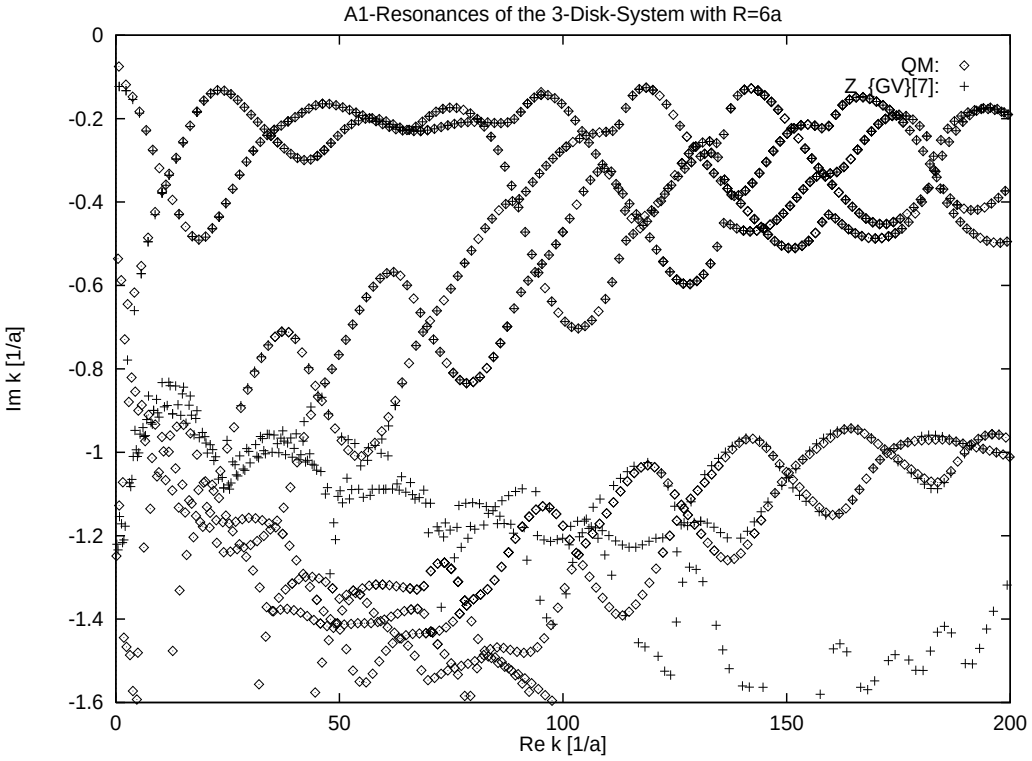

Figure 5.3: The A_1 resonances of the 3-disk system with $R : a = 6$. The exact quantum mechanical resonances calculated by A. Wirzba are denoted by a diamond. The semiclassical Gutzwiller-Voros resonances are calculated up to the 7'th order in the curvature expansion and are denoted by crosses. It should be noted that by inclusion of longer orbits in the calculation, the picture becomes much worse, as the Gutzwiller-Voros zeta function is only an asymptotic series and the cycle expansion start diverging. The data are from A. Wirzba.

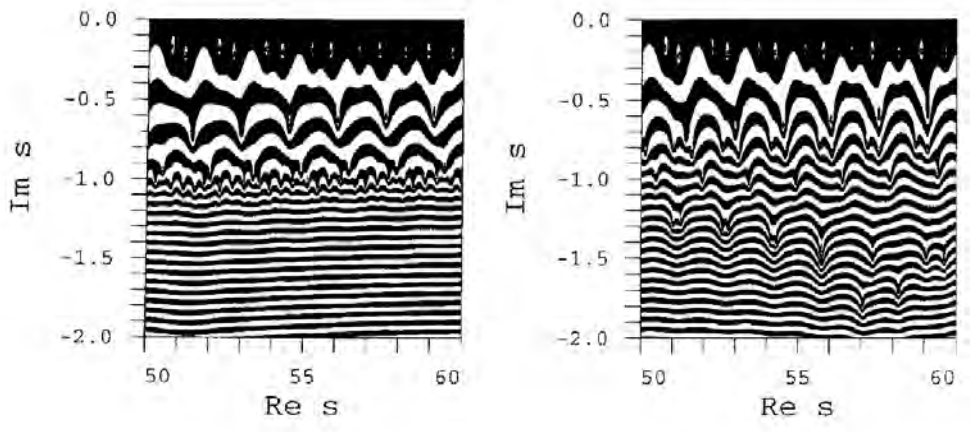

Figure 5.4: Complex s plane contour plot comparison of (a) the Gutzwiller-Voros zeta function $\log|Z_{qm}(s)|$ with (b) the quantum Fredholm determinant $\log|F_{qm}(s)|$. The border of the convergence of the Gutzwiller-Voros zeta function agrees with the location of the abscissa of absolute convergence, given by the $\hat{F}_{1/2}$ leading eigenvalue at $\mathrm{Re}(s) = 0$, $\mathrm{Im}(s) = -0.699110157151\ldots$. The quantum Fredholm determinant can be continued at least a factor 2 further down in the complex plane. 3-disk repeller, $R : a = 6 : 1$, A_1 subspace, maximal cycle length $n = 8$.

is

$$i\hbar\frac{\partial\psi}{\partial t} = -\frac{\hbar^2}{2}\Delta\psi + U(q)\psi, \tag{5.6}$$

where Δ is the Laplace operator and $\psi(q,t)$ is the wave function. In the limit $\hbar \to 0$ the solution of this equation is given by the quasi-classical approximation which is an asymptotic solution of the form

$$\psi(q,t) = \varphi(q,t)e^{iS(q,t)/\hbar}, \tag{5.7}$$

where the amplitude $\varphi(q,t)$ and the phase $S(q,t)$ are smooth real functions on some bounded region of the configuration space. The reason for the changed notation as compared to the WKB ansatz (4.4), is that we shall here keep the wave function as one single term of the WKB form and not as a sum of contributions from different branches as in the case of the Van Vleck propagator. This is also what lies in the notion of a quasi-classical wave function. Substituting (5.7) into the Schrödinger equation and expanding the equation to zeroth and first order in $\hbar$ we get partial differential equations for the amplitude and the phase with initial conditions $\varphi(q,0) = \varphi_0(q)$ and $S(q,0) = S_0(q)$ respectively. The equations are

$$\frac{\partial\varrho}{\partial t} + div\,(\varrho\nabla S) = 0, \tag{5.8}$$

$$\frac{\partial S}{\partial t} + H(q,\nabla S) = 0, \tag{5.9}$$

where $\varrho(q,t) = \varphi^2(q,t)$ and $H(q,p)$ is the Hamilton function. Equation (5.9) is the classical Hamilton-Jacobi equation. It is an autonomous first order partial differential equation whose solution corresponding to an initial $S(q,0) = S_0(q)$, can be given independently of (5.8). Equation (5.8) is the continuity equation known from e.g. fluid or electro dynamics. As we see it is not an independant equation since it is driven by the solution of (5.9).

From the theory of first order PDE's [2] we know that their solutions lead to *ordinary* differential equations. The Hamilton-Jacobi equation for instance leads to the well known Hamilton differential equations of motion

$$\begin{aligned} \dot{q} &= \frac{\partial H(q,p)}{\partial p}, \\ \dot{p} &= -\frac{\partial H(q,p)}{\partial q}, \end{aligned} \tag{5.10}$$

where the new variable

$$p = \nabla S(q,t)$$

has been introduced.

When we take the wievpoint of the PDE description we evolve the whole function $S(q,t)$ and compute its gradient at a given point q_0. This requires information about the behavior of the function $S(q,t)$ in the vicinity of q_0 and cannot be recovered from the value of $S(q_0,t)$ alone. In the ODE description however, we evolve both q and the gradient $p = \nabla S(q,t)$. At a given time we therefore do not have to compute the gradient from $S(q,t)$ since the evolution is *local* in the (q,p) space. The final solution of the partial differential equation can be constructed from the ODE description as

$$S(q',t) = S(q,0) + \int_0^t L(q(\tau), \dot{q}(\tau)) d\tau, \tag{5.11}$$

where the Lagrange function is integrated along the phase space trajectory with

$$q' = q(t), q = q(0), \nabla S(q',t) = p(t), \nabla S(q,0) = p(0).$$

In general there exists only one such trajectory.

Next we consider the 'local' solution of the continuity equation (5.8). At a given starting point q_0 the momentum is given by $p_0 = \nabla S_0(q_0)$, and the amplitude of the wave function is $\varphi_0(q)$. During time t the coordinate q_0 evolves to $q(t)$ and p_0 to $p(t)$ following the full Hamiltonian flow. Using probability conservation the new amplitude can be derived as follows: First we take an infinitesimal initial d dimensional oriented volume $V(q_0)$ around q_0 in configuration space. In time t this volume evolves to the infinitesimal orientated volume $V(q(t))$ around $q(t)$ according to the full Hamiltonian flow. Applying the probability conservation the new amplitude is given by

$$\varphi(q(t)) = \pm \left(\frac{V(q(t))}{V(q(0))} \right)^{-1/2} \varphi_0(q_0), \tag{5.12}$$

where the sign ± 1 reflects the ambiguity of the transformation from the density ϱ to φ. The ratio of volumes is independent of the way we specify the initial infinitesimal volume. To determine the volume ratio, we specify an initial directed parallelepiped around q_0 with edges given by d independent infinitesimal vectors $\delta\mathbf{q}_1, \delta\mathbf{q}_2, \ldots \delta\mathbf{q}_d$. In time t these vectors are transformed into $\delta\mathbf{q'}_1, \delta\mathbf{q'}_2, \ldots \delta\mathbf{q'}_d$ by the flow. We then note that the initial point (q_0, p_0) and the set of initial vectors $\delta\mathbf{q}$ is not enough to specify uniquely the image vectorsi $\delta\mathbf{q}'$. This of course is due to the fact that we have not specified the initial momenta $\delta\mathbf{p}$ of the points in the volume, and that this is evolved by the full phase flow. The initial function $S_0(q)$ however determines a set $\delta\mathbf{p}_1, \delta\mathbf{p}_2, \ldots \delta\mathbf{p}_d$ of initial momentum vectors through the second derivative matrix:

$$\delta\mathbf{p} = \mathbf{M}\delta\mathbf{q}, \quad \mathbf{M}_{ji} = \frac{\partial^2 S_0(q)}{\partial q_j \partial q_i}, \tag{5.13}$$

which we hereafter call the *curvature matrix*. The initial curvature matrix $\mathbf{M}_0$ is therefore an important initial condition, and we are able to compute the image of the volume only by specifying it. The vector $(\delta\mathbf{q}_i, \delta\mathbf{p}_i)$ is transformed by the Jacobi matrix

$$\begin{aligned} \delta\mathbf{q'}_i &= \mathbf{J}_{qq}\delta\mathbf{q}_i + \mathbf{J}_{qp}\delta\mathbf{p}_i, & (5.14)\\ \delta\mathbf{p'}_i &= \mathbf{J}_{pq}\delta\mathbf{q}_i + \mathbf{J}_{pp}\delta\mathbf{p}_i, & (5.15)\\ & & (5.16) \end{aligned}$$

where the subscripts q and p denote the corresponding $[d \times d]$ submatrices of the full $[2d \times 2d]$ Jacobian. The Jacobian is determined by the initial condition (q_0, p_0) and can be computed as a time ordered integral along the phase space trajectory

$$\mathbf{J}(q,p,t) = \mathrm{T}\exp\left\{\int_0^t d\tau \mathbf{D}^2 H(q(\tau), p(\tau))\right\}, \tag{5.17}$$

where $\mathbf{D}^2 H(q,p)$ denotes the second symplectic derivative matrix

$$\begin{aligned} \mathbf{D}^2 H &= \begin{pmatrix} \frac{\partial^2 H}{\partial q_i \partial p_j} & \frac{\partial^2 H}{\partial p_i \partial p_j} \\ -\frac{\partial^2 H}{\partial q_i \partial q_j} & -\frac{\partial^2 H}{\partial q_i \partial p_j} \end{pmatrix} \\ &\equiv \mathbf{D}^2 H \end{aligned}$$

of the Hamiltonian and T is the time ordering operator. The derivation of equation (5.17) is sketched in appendix 9.1. The curvature matrix of the function $S(q,t)$ around $q(t)$ relates between the infinitesimal vectors as in (5.13)

$$\delta\mathbf{p}' = \mathbf{M}'\delta\mathbf{q}', \quad \mathbf{M}'_{ji} = \frac{\partial^2 S(q',t)}{\partial q_j \partial q_i}. \tag{5.18}$$

From (5.13) and (5.18), we can eliminate the vectors $\delta\mathbf{p}_i$ and $\delta\mathbf{p}'_i$ and get relations between the initial and final infinitesimal configuration vectors and

the curvature matrices

$$\delta\mathbf{q}' = (\mathbf{J}_{qq} + \mathbf{J}_{qp}\mathbf{M})\delta\mathbf{q}, \tag{5.19}$$

$$\mathbf{M}' = (\mathbf{J}_{pq} + \mathbf{J}_{pp}\mathbf{M})(\mathbf{J}_{qq} + \mathbf{J}_{qp}\mathbf{M})^{-1}. \tag{5.20}$$

From the first relation it immediately follows that the volume ratio is given by

$$\frac{V(q')}{V(q_0)} = \det(\mathbf{J}_{qq} + \mathbf{J}_{qp}\mathbf{M}). \tag{5.21}$$

The second relation is a recursion relation for $\mathbf{M}$ which can be considered as the matrix generalization of the usual rational fraction transformation. Furthermore equation (5.20) allows us to derive a differential equation for $\mathbf{M}(t)$, which yields

$$\dot{\mathbf{M}} = -\left(\frac{\partial^2 H}{\partial q \partial q} + \mathbf{M}\frac{\partial^2 H}{\partial p \partial q} + \frac{\partial^2 H}{\partial q \partial p}\mathbf{M} + \mathbf{M}\frac{\partial^2 H}{\partial p \partial p}\mathbf{M}\right), \tag{5.22}$$

The derivation of this equation is also sketched in appendix 9.1. As we see equation(5.22) is driven since the second partial derivatives of the Hamilton function should be computed along the phase space trajectory. If we solve this differential equation along the phase space trajectory the volume ratio can be written as an integral along the phase space and $\mathbf{M}(t)$ trajectory (see appendix 9.1 for the derivation):

$$\frac{V(q')}{V(q_0)} = \exp\left\{\int_0^t \mathrm{Tr}[\frac{\partial^2 H}{\partial p \partial q} + \frac{\partial^2 H}{\partial p \partial p}\mathbf{M}]d\tau\right\} \tag{5.23}$$

The square root of the volume ratio is then also given by an integral:

$$\left(\frac{V(q')}{V(q_0)}\right)^{-1/2} = \exp\left\{-\frac{1}{2}\int_0^t \mathrm{Tr}\left[\frac{\partial^2 H}{\partial p \partial q} + \frac{\partial^2 H}{\partial p \partial p}\mathbf{M}\right]d\tau\right\}. \tag{5.24}$$

The computation of this expression requires some care when the solution of the differential equation (5.22) is singular. Close to a singularity, where

$$\mathbf{M}(t \to t^c) = \infty,$$

we can neglect the non leading terms from (5.22) and use the solution of

$$\dot{\mathbf{M}} = -\mathbf{M}\frac{\partial^2 H}{\partial p \partial p}\mathbf{M}. \tag{5.25}$$

The second derivative matrix can be decomposed into combinations of dyads and their eigenvalues in the usual way

$$\frac{\partial^2 H}{\partial p \partial p} = \sum_{i=1}^{d} \lambda_i \mathbf{D}_i, \quad \mathbf{D}_i\mathbf{D}_j = \delta_{ij}\mathbf{D}_j. \tag{5.26}$$

where $\mathbf{D}_j$ is the matrix constructed by the matrix product of the j'th right and left eigenvectors of $\partial^2 H/\partial p^2$: $\mathbf{D}_j = \mathbf{e}_j^{right}\mathbf{e}_j^{left}$.

The solution close to the singularity can be a linear combination of some of these dyads corresponding to singular directions l:

$$\mathbf{M}(t) = \frac{1}{t - t^c}\sum_{l=1}^{R}\frac{1}{\lambda_l}\mathbf{D}_l, \tag{5.27}$$

where R is the number of singular directions. The time ordered integral close to the singularity is then dominated by

$$\left(\frac{V(q(t^c_{+0}))}{V(q(t^c_{-0}))}\right)^{-1/2} = \exp\left(-\frac{1}{2}\int_{t_c-0}^{t_c+0}\frac{R}{\tau - t_c}d\tau\right). \tag{5.28}$$

This integral can be computed by adding infinitesimal imaginary value $i\epsilon$ to t^c and taking the $\epsilon \to 0$ limit

$$\left(\frac{V(q(t^c_{+0}))}{V(q(t^c_{-0}))}\right)^{-1/2} = \exp(i\pi(R/2)). \tag{5.29}$$

Between two singular points the time ordered integral is positive and gives the absolute value of the volume ratio. Notice that R counts the number of rank reductions of the matrix $\mathbf{M}$ along the classical path, and it is also a function on the initial condition $\mathbf{M}_0$.

We now have the necessary ingredients to describe the time evolution of a quasi-classical wave function. The wave function at time t becomes

$$\psi(q',t) = \varphi(q',t)e^{iS(q',t)/\hbar} = \pm\left(\frac{V(q')}{V(q_0)}\right)^{-1/2} e^{i\int_0^t Ld\tau/\hbar}\varphi_0(q_0)e^{iS_0(q_0)/\hbar} \tag{5.30}$$

where q_0 is the starting point of a classical trajectory with initial momentum $\nabla S_0(q_0)$ which ends up in q after time t with momentum $\nabla S(q,t)$, and the volume ratio is determined by the curvature matrix $\mathbf{M} = \partial_i\partial_j S(q,0)$. We note again that in contrast to the solution of the initial value problem in the WKB theory (4.14), we here only get one contribution to the quasi-classical wave function at time t.

5.2.1 Time evolution

We are now in a position to express the volume ratio and the momentum by the second and first derivatives of the minimal action between q' and q. In this way we recover the usual Van Vleck propagator. However, from equation (5.30) we see that the wave amplitude φ at time t and at coordinate q' is determined

by the amplitude at $t = 0$ at coordinate q. In calculations involving the Van Vleck operator kernel this nice property is lost, and we have to compute lots of trajectories to compute the volume ratio and we have to know the whole initial wave function too. However we have a better option. We can keep track of the variables p and $\mathbf{M}$ along only one trajectory and compute (5.11) and the volume ratio (5.24). This means that the evolution takes place on the extended $(q, p, \mathbf{M})$ space. We can introduce classical density functions $\tilde{\psi}$ defined on this space. The wave function then corresponds to the special function

$$\tilde{\psi}(q, p, \mathbf{M}, t) = \psi(q, t)\delta(p - \nabla S(q, t))\delta\left(\mathbf{M} - \frac{\partial^2 S(q, t)}{\partial q_j \partial q_i}\right). \tag{5.31}$$

The evolution of a general classical density function on the extended space according to (5.30) can be rewritten in terms of a classical transfer operator

$$\tilde{\psi}(q', p', \mathbf{M}', t) = \int dq dp d\mathbf{M} \mathcal{L}(q', p', \mathbf{M}', t \mid q, p, \mathbf{M}, 0)\tilde{\psi}(q, p, \mathbf{M}, 0), \tag{5.32}$$

with the kernel

$$\begin{aligned} e^{i\pi\nu + \int_0^t d\tau \frac{iL}{\hbar} + \frac{1}{2}\mathrm{Tr}\left\{\frac{\partial^2 H}{\partial p \partial q} + \frac{\partial^2 H}{\partial p \partial p}\mathbf{M}\right\}} &\times \delta(q' - q^t(q, p)) \times \\ \delta(p' - p^t(q, p)) &\times \delta(\mathbf{M}' - \mathbf{M}^t(q, p, \mathbf{M})), \end{aligned} \tag{5.33}$$

where $q^t(q, p)$, $p^t(q, p)$ and $\mathbf{M}^t(q, p, \mathbf{M})$ denote the evolution of q, p and $\mathbf{M}$ from the initial coordinates q,$p = \nabla S_0(q)$ and $\mathbf{M} = \partial_i \partial_j S_0(q)$ during the time t, and $\nu = N + R/2$. The integrals should be computed along the full trajectory, and also the number of rank reductions R and the number of orientation changes N. We note that the sign of the trace integral in the exponent has changed compared to the sign in (5.24). This arises as the integration over $p, \mathbf{M}$ and q picks up an additional volume ratio in the denominator, and the final expression should therefore be multiplied with the square root of the volume ratio in the numerator to give the right result as in (5.30). The derivation of this is shown in appendix 9.1.

We also note that the above evolution operator or kernel is *multiplicative*, since the delta functions ensure that the operator connects coordinates, which are connected by the classical dynamics, and give the correct amplitude. This operator can evolve densities, which are not of the form (5.31), and therefore we can expect that only a part of its spectrum has relevance to semiclassics.

5.3 Derivation of the trace integral

In this section we consider how the trace integration of the evolution operator introduced above, can be performed by considering the generalized rational fraction transformation (5.20) that governs the evolution of the curvature matrix. An alternative derivation of this result where we follow explicitely the

Lagrangian manifolds around the periodic orbit, is given in appendix 9.1. Here we first find explicitely the periodic $\mathbf{M}$ solutions of the map, which gives us the solution to the second order of the Hamilton Jacobi equation in the neighbourhood of a periodic orbit. Next we look at the symplectic structure of the flow which imposes the same restriction on the number of periodic $\mathbf{M}$ solutions as was previously obtained. Finally we obtain the stabilities of the $\mathbf{M}$ solutions by "differentiating" the rational fraction transformation and inserting the periodic solutions of the curvature flow.

We are interested in the trace of the evolution operator $\mathcal{L}^t$ in (9.39)

$$\begin{aligned} \mathrm{tr}\mathcal{L}^t &= \int dqdpd\mathbf{M}\delta(q-q^t)\delta(p-p^t)\delta(\mathbf{M}-\mathbf{M}^t) \\ &\times \exp\left(i\pi\nu + \int_0^t d\tau \frac{iL}{\hbar} + \frac{1}{2}\mathrm{Tr}\{H_{pq}+H_{pp}\mathbf{M}\}\right). \end{aligned} \tag{5.34}$$

Following the strategy in section 3.1 we introduce longitudinal $\mathbf{x}_\parallel$ and perpendicular $\mathbf{x}_\perp$ coordinates along the total $\mathbf{x}=(q,p,\mathbf{M})$ flow to evaluate the contribution from a prime periodic orbit to the trace. In the longitudinal direction we get

$$\int d\mathbf{x}_\parallel \delta_\parallel(\mathbf{x}-\mathbf{x}^t) = T_p \sum_{r=1}^{\infty} \delta(t-rT_p) \tag{5.35}$$

where T_p is the period of the prime periodic orbit. In the perpendicular direction we get

$$\int d\mathbf{x}_\perp \delta_\perp(\mathbf{x}-\mathbf{x}^{rT_p}) = \frac{1}{|\det(\mathbf{1}-\hat{\mathbf{J}}_p^r)|} \tag{5.36}$$

where $\hat{\mathbf{J}}_p$ is the transverse stability matrix, $\mathbf{u}(t+T_p)=\hat{\mathbf{J}}_p\mathbf{u}(t)$ of the entire flow. Since $\frac{\partial q^t}{\partial \mathbf{M}}=\frac{\partial p^t}{\partial \mathbf{M}}=0$ it has the structure

$$\det \hat{\mathbf{J}}_p = \begin{bmatrix} \mathbf{J}_{tr} & 0 \\ * & \mathbf{J}_{\mathbf{M}} \end{bmatrix} \tag{5.37}$$

and since this is block diagonalizable the determinant splits up into a product of the usual transverse determinant and a determinant corresponding to the $\mathbf{M}$ flow

$$\det(\mathbf{1}-\hat{\mathbf{J}}_p^r) = \det(\mathbf{1}-\mathbf{J}_p^r)\cdot\det(\mathbf{1}-\mathbf{J}_{\mathbf{M}p}^r). \tag{5.38}$$

We can then write the trace in a form similar to the one in [15]

$$\mathrm{Tr}\mathcal{L}^t = \sum_p T_p \sum_{r=1}^{\infty} \frac{\delta(t-rT_p)e^{iS_p(E)r/\hbar}}{|\det(\mathbf{1}-\mathbf{J}_p^r)|}\Delta_{p,r}, \tag{5.39}$$

with

$$\Delta_{p,r} = \sum_{\mathbf{M}^{rT_p}=\mathbf{M}} \frac{e^{\frac{1}{2}\int_0^{rT_p}(H_{pq}+H_{pp}\mathbf{M})d\tau}}{|\det(\mathbf{1}-\mathbf{J}_{\mathbf{M}p}^r)|} \tag{5.40}$$

The related spectral (or Fredholm) determinant $F(k)$ can be obtained by observing that the Laplace transform of the trace

$$\mathrm{Tr}\mathcal{L}(k) \quad = \quad \int_{0^+}^{\infty} dt\, e^{kt} \mathrm{Tr}\, \mathcal{L}^t, \tag{5.41}$$

is a logarithmic derivative $\mathrm{Tr}\mathcal{L}(k) = -\frac{d}{dk} \log F(k)$

$$F(k) \quad = \quad \exp\left(- \sum_{p,r} \frac{e^{i\pi\nu r + iT_p k r}}{r|\det(\mathbf{1} - \mathbf{J}_{\mathbf{M}_p^r})|} \Delta_{p,r} \right). \tag{5.42}$$

In the following we shall refer to (5.42) as the Vattay determinant. The Vattay determinant is very similar in shape to the classical Fredholm determinant (3.9). The new thing we have to calculate is the curvature trace (9.28).

The first point in obtaining (9.28) is then to find the periodic solutions of the $\mathbf{M}$ flow, and evaluate their stabilities. Next we have to deal with the volume ratio, that is the integral

$$\exp\left(\int_0^t d\tau \frac{1}{2} \mathrm{Tr}\{H_{pq} + H_{pp}\mathbf{M}\} \right).$$

5.3.1 Finding periodic M solutions

In this section we derive a method of finding periodic solutions of the rational fraction transformation of the curvature matrix (5.20). The method is general and thus applies also to equations where the solution $\mathbf{M}$ is not required to be symmetric.

Let $\mathbf{A}, \mathbf{B}, \mathbf{C}, \mathbf{D}$ and $\mathbf{M}$ be $N \times N$ matrices. We consider the generalized rational fraction transformation map $f : \mathbf{M} \to \mathbf{M}'$ given by

$$f(\mathbf{M}) \quad = \quad (\mathbf{C} + \mathbf{D}\mathbf{M})(\mathbf{A} + \mathbf{B}\mathbf{M})^{-1}, \tag{5.43}$$

which we assume to be well defined. If we are looking for fixed points of the map $f(\mathbf{M}) = \mathbf{M}$ equation (5.43) results in a generalized second order equation

$$\mathbf{M}\mathbf{B}\mathbf{M} + \mathbf{M}\mathbf{A} - \mathbf{D}\mathbf{M} - \mathbf{C} = 0. \tag{5.44}$$

To solve the fixed point equation we start by taking an alternative approach to the map f. Consider the $2N \times 2N$ matrix $\mathbf{J}$ given by

$$\mathbf{J} = \begin{bmatrix} \mathbf{A} & \mathbf{B} \\ \mathbf{C} & \mathbf{D} \end{bmatrix} \tag{5.45}$$

and assume that it is diagonalizable:

$$\mathbf{\Delta} \quad = \quad \mathbf{T}\mathbf{J}\mathbf{T}^{-1}$$

where $\mathbf{\Delta}$ is a diagonal matrix. We note that if for instance $\mathbf{J}$ is the Jacobian of a nondegenerate Hamiltonian flow, then this diagonalization is indeed possible.

Now for any N by N matrix $\mathbf{M}$ and for any vector $\mathbf{x} \in R^N$ we can construct the $2N$ dimensional vector

$$\begin{bmatrix} \mathbf{x} \\ \mathbf{p} \end{bmatrix} = \begin{bmatrix} \mathbf{x} \\ \mathbf{Mx} \end{bmatrix}. \tag{5.46}$$

Mapping this by $\mathbf{J}$ results in

$$\begin{bmatrix} \mathbf{x}' \\ \mathbf{p}' \end{bmatrix} = \mathbf{J} \begin{bmatrix} \mathbf{x} \\ \mathbf{p} \end{bmatrix}$$

To find the fixed points of the map (5.43), we now show the following small theorem

Theorem 1 $\mathbf{M}$ *is a fixed point of the map* f *if and only if for all vectors* $\mathbf{x} \in R^N$

$$\begin{bmatrix} \mathbf{x}' \\ \mathbf{Mx}' \end{bmatrix} = \begin{bmatrix} \mathbf{A} & \mathbf{B} \\ \mathbf{C} & \mathbf{D} \end{bmatrix} \begin{bmatrix} \mathbf{x} \\ \mathbf{Mx} \end{bmatrix}. \tag{5.47}$$

Note that the curvature matrix is the same on both sides of the equality sign.

Proof

If $\mathbf{M}$ is a fixed point of the equation (5.43) we have

$$\begin{aligned} \begin{bmatrix} \mathbf{A} & \mathbf{B} \\ \mathbf{C} & \mathbf{D} \end{bmatrix} \begin{bmatrix} \mathbf{x} \\ \mathbf{Mx} \end{bmatrix} &= \begin{bmatrix} (\mathbf{A}+\mathbf{BM})\mathbf{x} \\ (\mathbf{C}+\mathbf{DM})\mathbf{x} \end{bmatrix} \\ &= \begin{bmatrix} \mathbf{x}' \\ (\mathbf{C}+\mathbf{DM})(\mathbf{A}+\mathbf{BM})^{-1}\mathbf{x}' \end{bmatrix} \\ &= \begin{bmatrix} \mathbf{x}' \\ \mathbf{Mx}' \end{bmatrix} \end{aligned} \tag{5.48}$$

so that the condition is fulfilled.

On the other hand: if the condition (5.47) is fulfilled we have

$$\begin{aligned} \mathbf{Mx}' &= \mathbf{M}(\mathbf{A}+\mathbf{BM})\mathbf{x} \\ &= (\mathbf{C}+\mathbf{DM})\mathbf{x} \end{aligned} \tag{5.49}$$

which is equivalent to

$$\mathbf{M}(\mathbf{A}+\mathbf{BM}) = (\mathbf{C}+\mathbf{DM}) \tag{5.50}$$

which gives

$$\mathbf{M} = (\mathbf{C}+\mathbf{DM})(\mathbf{A}+\mathbf{BM})^{-1} \tag{5.51}$$

implying

$$f(\mathbf{M}) = \mathbf{M} \quad \square \tag{5.52}$$

Now to use the theorem we can multiply by the diagonalization matrix $\mathbf{T}$ on both sides of the condition (5.47). This yields

$$\mathbf{T}\begin{bmatrix} \mathbf{x}' \\ \mathbf{M}\mathbf{x}' \end{bmatrix} = \mathbf{T}\mathbf{J}\mathbf{T}^{-1}\mathbf{T}\begin{bmatrix} \mathbf{x} \\ \mathbf{M}\mathbf{x} \end{bmatrix}, \tag{5.53}$$

which implies

$$\begin{bmatrix} \tilde{\mathbf{x}}' \\ \tilde{\mathbf{M}}\tilde{\mathbf{x}}' \end{bmatrix} = \begin{bmatrix} \tilde{\mathbf{A}} & 0 \\ 0 & \tilde{\mathbf{D}} \end{bmatrix}\begin{bmatrix} \mathbf{x} \\ \tilde{\mathbf{M}}\tilde{\mathbf{x}} \end{bmatrix}, \tag{5.54}$$

where we introduced the new coordinates

$$\begin{bmatrix} \tilde{\mathbf{x}} \\ \tilde{\mathbf{p}} \end{bmatrix} = \begin{bmatrix} \mathbf{T}_{qq} & \mathbf{T}_{qp} \\ \mathbf{T}_{pq} & \mathbf{T}_{pp} \end{bmatrix}\begin{bmatrix} \mathbf{x} \\ \mathbf{p} \end{bmatrix}. \tag{5.55}$$

(5.54) now shows that $\tilde{\mathbf{M}}$ is a fixed point for the map $\tilde{f}$ by the theorem. The new phase space coordinates $\tilde{\mathbf{x}}$ and $\tilde{\mathbf{p}}$ are given in terms of the old coordinates by

$$\begin{aligned} \tilde{\mathbf{x}} &= (\mathbf{T}_{qq} + \mathbf{T}_{qp}\mathbf{M})\mathbf{x}, \\ \tilde{\mathbf{p}} &= (\mathbf{T}_{pq} + \mathbf{T}_{pp}\mathbf{M})\mathbf{x}. \end{aligned} \tag{5.56}$$

Inserting this in the expression for $\tilde{\mathbf{p}} = \tilde{\mathbf{M}}\tilde{\mathbf{x}}$ we find

$$\tilde{\mathbf{M}} = (\mathbf{T}_{pq} + \mathbf{T}_{pp})(\mathbf{T}_{qq} + \mathbf{T}_{qp}\mathbf{M})^{-1}. \tag{5.57}$$

By the theorem we therefore have that $\mathbf{M}$ is a fixed point for f if and only if $\tilde{\mathbf{M}}$ is a fixed point of the transformed map $\tilde{f}$, which is obtained from the original map just by substituting in the new transformed tilde matrices from the transformed Jacobian. But

$$\tilde{f}(\tilde{\mathbf{M}}) = \tilde{\mathbf{D}}\tilde{\mathbf{M}}\tilde{\mathbf{A}}^{-1}, \tag{5.58}$$

where $\tilde{\mathbf{D}}$ and $\tilde{\mathbf{A}}$ now are diagonal so this is only a simple linear equation

$$\tilde{\mathbf{M}}_{ij} = \mu_{ij}\tilde{\mathbf{M}}_{ij}, \tag{5.59}$$

which can easily be solved. From the $\tilde{\mathbf{M}}$ solution we therefore finally get the $\mathbf{M}$ solution from (5.57) as

$$\mathbf{M} = (\tilde{\mathbf{M}}\mathbf{T}_{qp} - \mathbf{T}_{pp})^{-1}(\mathbf{T}_{pq} - \tilde{\mathbf{M}}\mathbf{T}_{qq}). \tag{5.60}$$

If we suppose that the eigenvalues of the Jacobian are non degenerate, i.e. $\mu_{ij} \neq 1$, we therefore only have the trivial solution for $\tilde{\mathbf{M}}$:

$$\tilde{\mathbf{M}} = \mathbf{0} \tag{5.61}$$

which finally gives the $\mathbf{M}$ solution

$$\mathbf{M} = -\mathbf{T}_{pp}^{-1}\mathbf{T}_{pq} \tag{5.62}$$

A couple of examples of the solution of second order matrix equations by use of (5.62) are given in appendix 9.1.

5.3.2 Symplectic matrices

By the above procedure we get $K_{2N,N} = (2N)!/N!^2$ periodic solutions of the rational fraction transformation, which are too many since the matrix $\mathbf{M}$ should fulfill certain conditions imposed by the intrinsic nature of the Hamiltonian flow. In this section we show which restrictions the symplectic structure of the Jacobian imposes on the curvature matrix.

Let ω be the *symplectic* $[2N \times 2N]$ bilinear invariant

$$\omega = \begin{bmatrix} \mathbf{0} & \mathbf{1} \\ -\mathbf{1} & \mathbf{0} \end{bmatrix}. \tag{5.63}$$

A matrix $\mathbf{A}$ is said to be symplectic if

$$\mathbf{A}^t \omega \mathbf{A} = \omega. \tag{5.64}$$

Writing $\mathbf{A}$ as four block matrices

$$\mathbf{A} = \begin{bmatrix} a_{11} & a_{12} \\ a_{21} & a_{22} \end{bmatrix}, \tag{5.65}$$

the condition (5.64) immediately implies the following rules for the individual block matrices in order that the total matrix should be symplectic

$$a_{11}^t a_{21} = a_{21}^t a_{11}, \qquad \text{and} \qquad a_{12}^t a_{22} = a_{22}^t a_{12}, \tag{5.66}$$

$$a_{11}^t a_{22} - a_{21}^t a_{12} = a_{12}^t a_{21} - a_{22}^t a_{11} = 1. \tag{5.67}$$

Further more we get from (5.64) that

$$\mathbf{A}^{-1} = -\omega \mathbf{A}^t \omega, \tag{5.68}$$

since $\omega^{-1} = -\omega$, which implies

$$a_{21} a_{22}^t = a_{22} a_{21}^t \text{ , and } a_{11} a_{12}^t = a_{12} a_{11}^t. \tag{5.69}$$

5.3.3 The general M solution

In section 5.3.1 we saw that the general solution of the fixed point equation for the curvature matrix was given by

$$\mathbf{M} \quad = \quad (\tilde{\mathbf{M}}\mathbf{T}_{qp} - \mathbf{T}_{pp})^{-1}(\mathbf{T}_{pq} - \tilde{\mathbf{M}}\mathbf{T}_{qq}).$$

If $\mathbf{J}$ is a symplectic matrix and the diagonalizing matrix $\mathbf{T}$ is also a symplectic matrix, then the diagonalization $\mathbf{\Delta}$ of $\mathbf{J}$ is also symplectic. Writing the diagonalized Jacobian as

$$\mathbf{T}\mathbf{J}\mathbf{T}^{-1} = \begin{bmatrix} \mathbf{\Delta}_A & \mathbf{\Delta}_B \\ \mathbf{\Delta}_C & \mathbf{\Delta}_D \end{bmatrix},$$

this however implies that

$$\mathbf{\Delta}_A = \mathbf{\Delta}_D^{-1}, \tag{5.70}$$

so that the eigenvalues belonging to each other must be placed in the same order in the diagonal of $\mathbf{\Delta}_A$ and $\mathbf{\Delta}_D$ respectively. Assuming that we are dealing with Hamiltonian hyperbolic systems the linear fixed point equation (5.58) for $\tilde{\mathbf{M}}$ then becomes

$$\tilde{m}_{ij} = \lambda_i^2 \tilde{m}_{ij}, \tag{5.71}$$

where $\lambda_i \neq 1$ and hence the equation has only the solution

$$\tilde{\mathbf{M}} = \mathbf{0}. \tag{5.72}$$

This means that the solution in the original coordinate system will have the form

$$\mathbf{M} = -\mathbf{T}_{pp}^{-1}\mathbf{T}_{pq}, \tag{5.73}$$

which follows from (5.60). From the results in (5.69) we obtain

$$\begin{aligned} \mathbf{M}(\mathbf{M}^{-1})^t &= \mathbf{T}_{pp}^{-1}\mathbf{T}_{pq}((\mathbf{T}_{pp}^{-1}\mathbf{T}_{pq})^{-1})^t \\ &= \mathbf{T}_{pp}^{-1}\mathbf{T}_{pq}\mathbf{T}_{pp}^t(\mathbf{T}_{pq}^{-1})^t \\ &= \mathbf{T}_{pp}^{-1}\mathbf{T}_{pp}\mathbf{T}_{pq}^t(\mathbf{T}_{pq}^{-1})^t \\ &= \mathbf{1}, \end{aligned} \tag{5.74}$$

so that

$$\begin{aligned} \mathbf{M} &= -\mathbf{T}_{pp}^{-1}\mathbf{T}_{pq} \\ &= \mathbf{M}^t, \end{aligned} \tag{5.75}$$

and hence the curvature matrix is symmetric as a consequence of the symplectic structure. This implies that $(\mathbf{q}, \mathbf{M}\mathbf{q})$ does in fact span a Lagrangian manifold as it should since $\mathbf{M}$ is the symmetric second derivative matrix of the phase function $S(x,t)$ (see appendix 9.1).

The next question is how many symmetric $\mathbf{M}$ solutions are there? To get the answer we have to study the diagonalization matrix $\mathbf{T}$. We know that $\mathbf{T}^{-1}$ have to contain the eigenvectors of $\mathbf{J}$ but it seems that we are free to permute them as we want as well as we have the possibility to scale the individual

eigenvectors arbitrarily. As we shall see now the symplectic structure puts quite a restriction on this liberty. A permutation of the columns of $\mathbf{T}^{-1}$ can be performed by multiplication from the right by a permutation matrix $\mathbf{P}_\tau(\mathbf{a})$ that permutes the columns following the permutation τ and at the same time multiply the columns by the weighting vector $\mathbf{a} = (a_1, a_2, \ldots, a_{2N})$. Such a permutation matrix can be defined by

$$[\mathbf{P}_\tau(\mathbf{a})]_{ij} \quad = \quad \delta_{\tau(j),i} a_j. \tag{5.76}$$

For instance

$$\begin{bmatrix} 1 & a & 7 & e \\ 2 & b & 9 & f \\ 3 & c & 1 & g \\ 4 & d & 3 & h \end{bmatrix} \begin{bmatrix} 0 & 0 & a_3 & 0 \\ a_1 & 0 & 0 & 0 \\ 0 & a_2 & 0 & 0 \\ 0 & 0 & 0 & a_4 \end{bmatrix} = \begin{bmatrix} a_1 a & a_2 7 & a_3 1 & a_4 e \\ a_1 b & a_2 9 & a_3 2 & a_4 f \\ a_1 c & a_2 1 & a_3 3 & a_4 g \\ a_1 d & a_2 3 & a_3 4 & a_4 h \end{bmatrix}.$$

Similarly the rows can be permuted by multiplication from the left with permutation matrices. From the definition of $\mathbf{P}_\tau(\mathbf{a})$ it follows immediately that

$$\mathbf{P}_\tau^{-1}(\mathbf{a}) \quad = \quad \mathbf{P}_\tau^t(\mathbf{a}^{-1}), \tag{5.77}$$

where $\mathbf{a}^{-1}$ means $(a_1^{-1}, a_2^{-1}, \ldots, a_N^{-1})$, and superscript t denots the transposed matrix. The symplectic condition for a permutation matrix can be written

$$\mathbf{P}_\tau^t(\mathbf{a})\omega \quad = \quad \omega \mathbf{P}_\tau^{-1}(\mathbf{a}), \tag{5.78}$$

and using the relation (5.77) and writing the permutation matrix as the usual four block matrices we get

$$\begin{bmatrix} -\mathbf{P}_{21}^t(\mathbf{a}) & \mathbf{P}_{11}^t(\mathbf{a}) \\ -\mathbf{P}_{22}^t(\mathbf{a}) & \mathbf{P}_{12}^t(\mathbf{a}) \end{bmatrix} = \begin{bmatrix} \mathbf{P}_{12}^t(\mathbf{a}^{-1}) & \mathbf{P}_{22}^t(\mathbf{a}^{-1}) \\ -\mathbf{P}_{11}^t(\mathbf{a}^{-1}) & -\mathbf{P}_{21}^t(\mathbf{a}^{-1}) \end{bmatrix},$$

so that the condition for a permutation matrix to be symplectic is

$$-\mathbf{P}_{21}(\mathbf{a}) = \mathbf{P}_{12}(\mathbf{a}^{-1}), \tag{5.79}$$

and

$$\mathbf{P}_{11}(\mathbf{a}) = \mathbf{P}_{22}(\mathbf{a}^{-1}). \tag{5.80}$$

Since the columns in $\mathbf{T}^{-1}$ *must* contain the eigenvectors of the Jacobian, we see that the Jacobian can only be diagonalized by symplectic rotations if they are of the form

$$\tilde{\mathbf{T}} \quad = \quad \mathbf{P}\mathbf{T}, \tag{5.81}$$

where $\mathbf{T}$ is a symplectic matrix that diagonalizes $\mathbf{J}$, and $\mathbf{P}$ is a symplectic permutation matrix.

Now what is the significance of the local block matrices in $\mathbf{P}$? The blocks in the diagonal $\mathbf{P}_{11}$ and $\mathbf{P}_{22}$ simply permutes the local rows of $\mathbf{T}_{qq}, \mathbf{T}_{qp}$ and $\mathbf{T}_{pq}, \mathbf{T}_{pp}$ respectively. As we can write

$$\tilde{\mathbf{M}} = -(\mathbf{p}\mathbf{T}_{pp})^{-1}\mathbf{p}\mathbf{T}_{pq} = \mathbf{M},$$

we see that such a *local* permutation $\mathbf{p}$ does not change the $\mathbf{M}$ solution. However, the elements different from zero in $\mathbf{P}_{21}$ exchange rows in $\mathbf{T}_{pp}$ and $\mathbf{T}_{pq}$ with upper rows in $\mathbf{T}$ and hence change the $\mathbf{M}$ solution. Each row in $\mathbf{P}_{21}$ say, has then essentially two possible states: either it is a pure zero row, or it contains a '1'. The exact position of the '1' is not important since this can be shifted by a local permutation and thus does not alter the $\mathbf{M}$ solution. Since $\mathbf{P}_{21}$ has N rows each having two possible states there must be 2^N different solutions to the $\mathbf{M}$ fix point equation, which can be obtained from symplectic diagonalizations of the Jacobian.

By studying the symplectic structure we have thus found that there are 2^N symmetric periodic solutions to (5.20). A couple of examples where the solution formula (5.62) and the above considerations is applied to a symplectic matrix are given in appendix 9.1.

5.3.4 Stabilities of the periodic curvature solutions

Let us for now suppose that we have found the periodic solutions of the rational fraction transformation map f,

$$f(\mathbf{M}) = (\mathbf{C} + \mathbf{D}\mathbf{M})(\mathbf{A} + \mathbf{B}\mathbf{M})^{-1}, \tag{5.82}$$

i.e. the periodic curvature matrix solutions. We now would like to find the stabilities of the periodic solutions by using (5.82). This can be accomplished by variation of the map

$$f(\mathbf{M} + \delta\mathbf{M}) = f(\mathbf{M}) + Df(\delta\mathbf{M}) + \mathcal{O}(\|\delta\mathbf{M}^2\|), \tag{5.83}$$

where the so called *Frechet derivative* Df is just a linear map. For an alternative approach to the stability calculation see appendix 9.1. To simplify notation we introduce the two functions

$$\begin{aligned} N(\mathbf{M}) &= \mathbf{C} + \mathbf{D}\mathbf{M}, \\ D(\mathbf{M}) &= \mathbf{A} + \mathbf{B}\mathbf{M}, \end{aligned} \tag{5.84}$$

where N stands for the numerator, and D for the denominator. To obtain the Frechet derivative of the rational fraction transformation we proceed in the way of usual differentiation

$$\begin{aligned} f(\mathbf{M} + \delta\mathbf{M}) - f(\mathbf{M}) &= N(\mathbf{M} + \delta\mathbf{M})D^{-1}(\mathbf{M} + \delta\mathbf{M}) - N(\mathbf{M})D^{-1}(\mathbf{M}) \\ &= (N(\mathbf{M} + \delta\mathbf{M}) - N(\mathbf{M}))D^{-1}(\mathbf{M} + \delta\mathbf{M}) \\ &+ N(\mathbf{M})(D^{-1}(\mathbf{M} + \delta\mathbf{M}) - D^{-1}(\mathbf{M})), \end{aligned} \tag{5.85}$$

where in the last equation we have just subtracted and added the same term $N(\mathbf{M})D^{-1}(\mathbf{M}+\delta\mathbf{M})$.

If we now consider the first term, we obtain in the limit $\delta\mathbf{M} \to \mathbf{0}$ directly

$$1.term \;=\; \mathbf{D}\delta\mathbf{M}N^{-1}(\mathbf{M}). \tag{5.86}$$

For the denominator part in the second term we write

$$\begin{aligned} D^{-1}(\mathbf{M}+\delta\mathbf{M}) - D^{-1}(\mathbf{M}) &= D^{-1}(\mathbf{M}+\delta\mathbf{M})\{\mathbf{1} - \\ &\quad [D(\mathbf{M}+\delta\mathbf{M}) - D(\mathbf{M}) + D(\mathbf{M})]D^{-1}(\mathbf{M})\} \\ &= D^{-1}(\mathbf{M}+\delta\mathbf{M})\left[D(\mathbf{M}+\delta\mathbf{M}) - D(\mathbf{M})\right]D^{-1}(\mathbf{M}). \end{aligned}$$

In the limit $\delta\mathbf{M} \to \mathbf{0}$ this becomes

$$2.term \;=\; -D^{-1}(\mathbf{M})\mathbf{B}\delta\mathbf{M}D^{-1}(\mathbf{M}). \tag{5.87}$$

Gathering both terms we can write

$$f(\mathbf{M}+\delta\mathbf{M}) - f(\mathbf{M}) \;=\; \left(\mathbf{D} - N(\mathbf{M})D^{-1}(\mathbf{M})\mathbf{B}\right)\delta\mathbf{M}D^{-1}(\mathbf{M}) + \mathcal{O}(\|\delta\mathbf{M}^2\|), \tag{5.88}$$

so that the general expression for the derivative is

$$Df(\delta\mathbf{M}) \;=\; (\mathbf{D} - N(\mathbf{M})D^{-1}(\mathbf{M})\mathbf{B})\delta\mathbf{M}D^{-1}(\mathbf{M}). \tag{5.89}$$

Since the stabilities are robust to change of coordinates i.e. the fix point x for the map f has the same stability as the transformed fix point $g(x)$ of the map $\tilde{f} = g \odot f \odot g^{-1}$, we can calculate the stabilities in the basis where we have diagonalized the Jacobian matrix.

In the case where $\mathbf{M}$ is a fixed point of the map we get

$$\begin{aligned} Df(\delta\mathbf{M}) &= (\mathbf{D} - \mathbf{M}\mathbf{B})\delta\mathbf{M}D^{-1}(\mathbf{M}) \\ &= (\mathbf{D} - \mathbf{M}\mathbf{B})\delta\mathbf{M}(\mathbf{A} + \mathbf{B}\mathbf{M})^{-1}. \end{aligned} \tag{5.90}$$

And in the case where we have diagonalized $\mathbf{J}$ we therefore simply get

$$\begin{aligned} Df(\delta\mathbf{M}) &= \mathbf{D}\delta\mathbf{M}\mathbf{A}^{-1} \\ &= [\Lambda_i\Lambda_j\delta\mathbf{M}_{ij}], \end{aligned} \tag{5.91}$$

where $\mathbf{A}$ and $\mathbf{D}$ are diagonal. We note (5.91) is a *symmetric* matrix if the variation $\delta\mathbf{M}$ is itself symmetric. The eigenvariations can now be found from the equation

$$Df(\delta\mathbf{M}) \;=\; \tilde{\Lambda}\delta\mathbf{M}, \tag{5.92}$$

and for symmetric variations $\delta\mathbf{M}$ the $N(N+1)/2$ eigenvalues are read off as

$$\tilde{\Lambda}_i \;=\; \Lambda_i\Lambda_j, \quad i = 1,\ldots N \quad j = i,\ldots,N \tag{5.93}$$

since the matrices $\mathbf{A}$ and $\mathbf{D}$ are diagonal and fulfills $\mathbf{A}^{-1} = \mathbf{D}$ according to (5.70). The eigenvalues are thus given in terms of the original cycle stabilities.

The volume ratio

The only thing we miss in obtaining the general result for $\mathrm{Tr}\mathcal{L}$, is then to find the volume ratio (5.21)

$$\frac{V(q')}{V(q_0)} = \det(\mathbf{J}_{qq} + \mathbf{J}_{qp}\mathbf{M}). \tag{5.94}$$

To determine this, we note that for a given $\mathbf{M}$ (the periodic solutions) the matrix

$$\mathbf{j}_{\mathbf{M}} = \mathbf{J}_{qq} + \mathbf{J}_{qp}\mathbf{M}, \tag{5.95}$$

is the *configuration space Jacobian*, which governs the evolution of the projection of the total phase space flow on configuration space. The configuration space flow of course depends on the momentum also and to see that (5.95) is the right expression, we can look at the map given by the full phase space Jacobian

$$\begin{bmatrix} \mathbf{x}' \\ \mathbf{M}'\mathbf{x}' \end{bmatrix} = \begin{bmatrix} \mathbf{J}_{qq} & \mathbf{J}_{qp} \\ \mathbf{J}_{pq} & \mathbf{J}_{pp} \end{bmatrix} \begin{bmatrix} \mathbf{x} \\ \mathbf{M}\mathbf{x} \end{bmatrix}, \tag{5.96}$$

which tells us that local variations in configuration space $\delta\mathbf{q}$ maps into

$$\delta\mathbf{q}' = (\mathbf{J}_{qq} + \mathbf{J}_{qp}\mathbf{M})\delta\mathbf{q}. \tag{5.97}$$

The volume ratio (5.94) is therefore given by the product of the N eigenvalues λ_i of $\mathbf{j}_{\mathbf{M}}$. To find these eigenvalues let us first assume that we have found the corresponding eigenvectors $\mathbf{e}_1, \ldots, \mathbf{e}_N$. Then by constructing the full phase space vector $(\mathbf{e}_i, \mathbf{M}\mathbf{e}_i)$, and mapping this by the full phase space Jacobian $\mathbf{J}$ we obtain

$$\begin{aligned} \mathbf{J}\begin{bmatrix} \mathbf{e}_i \\ \mathbf{M}\mathbf{e}_i \end{bmatrix} &= \begin{bmatrix} (\mathbf{J}_{qq} + \mathbf{J}_{qp}\mathbf{M})\mathbf{e}_i \\ (\mathbf{J}_{pq} + \mathbf{J}_{pp}\mathbf{M})\mathbf{e}_i \end{bmatrix}, \\ &= \begin{bmatrix} (\mathbf{J}_{qq} + \mathbf{J}_{qp}\mathbf{M})\mathbf{e}_i \\ (\mathbf{J}_{pq} + \mathbf{J}_{pp}\mathbf{M})(\mathbf{J}_{qq} + \mathbf{J}_{qp}\mathbf{M})^{-1}\mathbf{e}_i' \end{bmatrix} \end{aligned} \tag{5.98}$$

but since $\mathbf{e}_i$ was assumed to be an eigenvector of $\mathbf{j}_{\mathbf{M}}$ corresponding to the *periodic* curvature solution $\mathbf{M}$ we just get

$$\mathbf{J}\begin{bmatrix} \mathbf{e}_i \\ \mathbf{M}\mathbf{e}_i \end{bmatrix} = \lambda_i \begin{bmatrix} \mathbf{e}_i \\ \mathbf{M}\mathbf{e}_i \end{bmatrix}, \tag{5.99}$$

which implies that λ_i must be the same as one of the full phase space eigenvalues ie. $\lambda_i = \Lambda_j$ for some j. Conversely it is easy to show (see appendix 9.1) that if we can write a full phase space eigenvector as $\mathbf{e} = (\delta\mathbf{q}, \tilde{\mathbf{M}}\delta\mathbf{q})$ for some $\tilde{\mathbf{M}}$, then this $\tilde{\mathbf{M}}$ will be a periodic solution of the curvature map (5.20). For each periodic $\mathbf{M}$ solution we therefore have N configuration space eigenvalues which are just given by the eigenvalues of the full phase space eigenvectors corresponding to the periodic solution $\mathbf{M}$ (see appendix 9.1). The volume ratio (5.94) is therefore just the product of the cycle stabilities corresponding to the given $\mathbf{M}$ solution.

These can be identified by noting that for a given $\mathbf{M}$ solution, the manifold spanned by $(\delta\mathbf{q}, \mathbf{M}\delta\mathbf{q})$ corresponds to a definite subset of the $2N$ phase space eigenvectors spanning the same (Lagrangian) manifold. For a detailled study of this correspondance we refer to appendix 9.1. The volume ratio after r repetitions of the cycle can now be written as

$$\frac{V(q^{rT_p})}{V(q)} = \prod_{i=1}^{N} |\Lambda_i^{-r}| \tag{5.100}$$

We are thus finally in a position where we can state the general result for the curvature trace (9.28). This reads

$$\begin{aligned}\Delta_{p,r} &= \int d\mathbf{M} e^{\int_0^{rT_p} d\tau \frac{1}{2}\mathrm{Tr}(H_{pq}+H_{pp}\mathbf{M})} \delta(\mathbf{M} - \mathbf{M}^{rT_p}(\mathbf{M})) \\ &= \sum_{l=1}^{2^N} \prod_{i_l=1}^{N} |\Lambda_{i_l}|^{-r/2} \prod_{j=i_l}^{N} |1 - \Lambda_j^r \Lambda_{i_l}^r|^{-1},\end{aligned} \tag{5.101}$$

where l labels the periodic $\mathbf{M}$ solutions. From this result we are now also able to evaluate the Vattay determinant (5.42) in any number of dimensions.

In the simple 2-dimensional case the above formula reduce to

$$\begin{aligned}\Delta_{p,r} &= \int d\mathbf{M} e^{\int_0^{rT_p} d\tau \frac{1}{2}\mathrm{Tr}\mathbf{M}} \delta(\mathbf{M} - \mathbf{M}^{rT_p}(\mathbf{M})) \\ &= \sum_{l=1}^{2} \prod_{i_l=1}^{1} |\Lambda_{i_l}|^{-r/2} \prod_{j=1}^{1} |1 - \Lambda_j^r \Lambda_{i_l}^r|^{-1} \\ &= \frac{|\Lambda_p^r|^{1/2}}{|1 - \Lambda_p^{-2r}|} + \frac{|\Lambda_p^r|^{-1/2}}{|1 - \Lambda_p^{2r}|} \\ &= \frac{|\Lambda_p^r|^{1/2}}{1 - \Lambda_p^{-2r}} + \frac{|\Lambda_p^r|^{-5/2}}{1 - \Lambda_p^{-2r}},\end{aligned} \tag{5.102}$$

which is the result obtained in [15].

5.4 Validity of the entire determinant

To examplify the validity of the new determinant we can try to do the same calculation as we did with the quantum Fredholm determinant in section 5.1.3. Evaluating the coefficients of the cycle expansion of the Vattay determinant at the leading zero $0.75831\ldots - i0.12282\ldots$ in the case of the 3-disk scatterer with $R : a = 6$ we get the results shown in figure 5.5. As we see the coefficients of the Vattay determinant displays a super exponential decay indicating that indeed there is no pole present. In the case of the quantum Fredholm determinant we see that the initial super exponential decay turns over in an exponential decay implying the presence of a pole.

The new spectral determinant has also recently been subject to a large number of investigations due to A. Wirzba [65]. This was due to the following observation: the Gutzwiller-Voros zeta function is an asymptotic series that

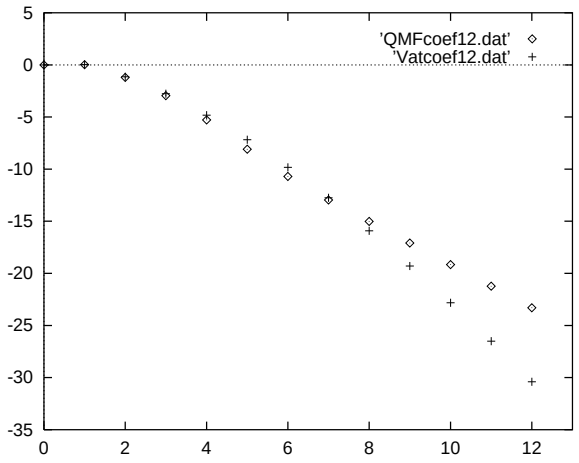

Figure 5.5: The logarithm (base 10) of the absolute value of the expansion coefficients C_n of the quantum Fredholm determinant ($\diamond$) and the Vattay determinant ($+$) versus cycle length n. The coefficients are evaluated at the leading zero $0.75831\ldots - i0.12282\ldots$ of the 3-disk system at $R : a = 6$.

mimics the behaviour of the quantum resonances up to a certain curvature order and then diverges. At curvature order 7 the leading as well as the subleading resonances are very well approximated as we saw in figure 5.3, but by inclusion of more periodic orbits the series diverges and the subleading resonances disappear. For the Vattay determinant the situation is much different. At curvature order 7 the leading resonances are found with high precision but in the domain of the subleading resonances a very complicated pattern of resonances occur, that does not resemble the correct resonances at all. However, if one continues and include more periodic orbits in the curvature expansion it turns out that at curvature order 12 (see figure 5.6) the resonance system breaks up into two different parts: the first part now also approximates the subleading resonances with good precision and the second part has nothing to do with the exact quantum resonances at all. These "fake" quantum resonances are presumably due to the fact that the Vattay evolution operator is not constructed specifically for quantum densities but is capable of evolving classical densities as well. We should therefore only expect a part of the resonance spectrum to be related to quantum mechanics. By inclusion of still more periodic orbits in the expansion we expect that the leading as well as the subleading resonances will stay put, since the spectral determinant should be an entire function in the complex plane.

Another problem occurs when one considers the "fake" resonances. Here it is hoped that these resonances can be filtered away by following the technique of Ref. [14]. The main idea here is that one can formally rewrite the Gutzwiller-Voros determinant as [15]

$$Z(k) \quad = \quad \frac{F_+(\frac{1}{2},k)F_-(\frac{7}{2},k)}{F_-(\frac{3}{2},k)F_+(\frac{5}{2},k)} \tag{5.103}$$

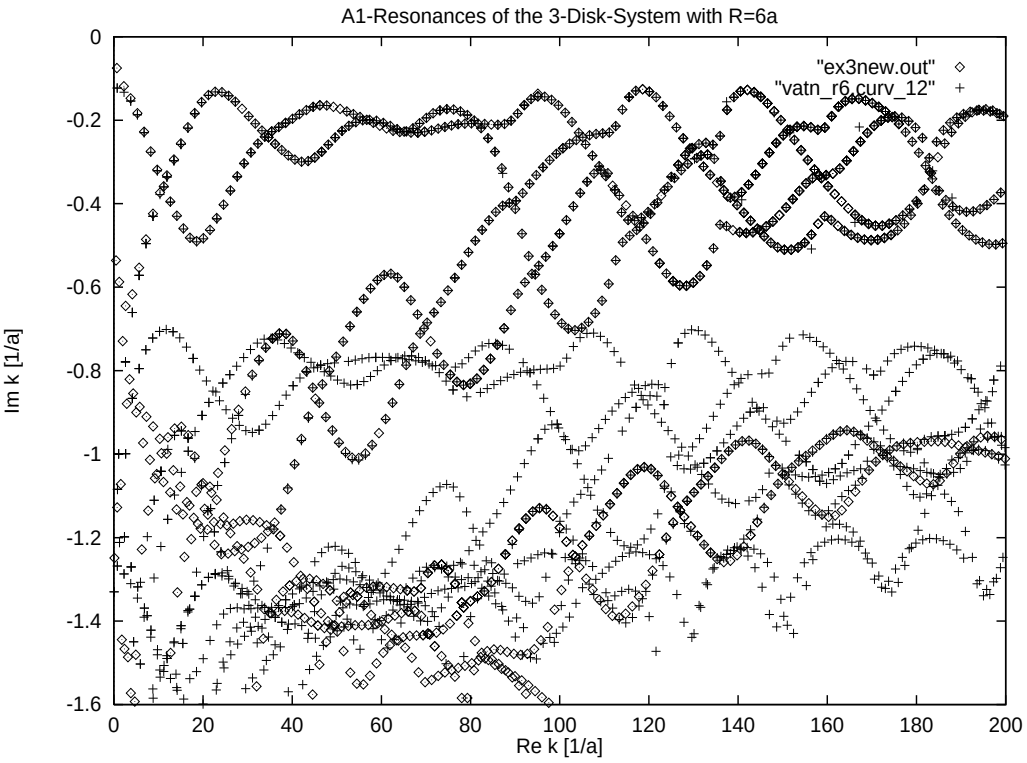

Figure 5.6: Scattering resonances of the A_1 representation of the $R : a = 6$ 3-disk system. The exact quantum resonances are denoted by diamonds, and the Vattay determinant resonances by crosses. In the cycle expansion of the Vattay determinant periodic orbits up to topological length 12 were used. The leading part of the spectrum is very well matched by the Vattay determinant. For the nonleading part of the spectrum the Vattay determinant also has the right quantum mechanical resonances, but furthermore yields a lot of unphysical resonances. It should be noted that the nonleading part of the spectrum is first obtained at curvature order 12 of the Vattay determinant. The data are from A. Wirzba.

where

$$F_\sigma(\beta,k) = \exp\left(-\sum_{p,r}\frac{\sigma_p^r}{r|\Lambda_p^r|}\frac{e^{rkT_p}}{(1-\Lambda_p^{-r})^2}\Delta_{p,r}(\beta)\right) \tag{5.104}$$

with $\sigma_p = \Lambda_p/|\Lambda_p|$ for F_-, and $\sigma_p = 1$ for F_+, and where only the first term in $\Delta_{p,r}$

$$\Delta_{p,r}(\beta) = \frac{|\Lambda_p^r|^{-\beta+1}}{1-\Lambda_p^{-2r}} + \frac{|\Lambda_p^r|^{\beta-3}}{1-\Lambda_p^{-2r}} \tag{5.105}$$

is included. The Gutzwiller-Voros zeta function is thus written as a ratio of entire functions [15], and the fake zeros of $F_+(\frac{1}{2},k)$ should be cancelled by the zeros of $F_-(\frac{3}{2},k)$. By numerical studies it turns out that the "fake" quantum resonances of $F_+(\frac{1}{2},k)$ almost coincide (up to a few digits) with the zeros of $F_-(\frac{3}{2},k)$, so that it is possible to extract the final approximation to the true quantum spectrum. The remaining problem is to find out why the cancellation of the fake zeros is not exact, which it should be as the determinants in the ratio should be entire. This might have to do with the interpretation of how a formal expansion like (5.103) should be carried out. Also numerical studies on the total scattering phase shift [65] indicates that the Gutzwiller-Voros zeta function is preferable to any other determinants or just the quantum zeta function. These problems are therefore still open. For the reader interested in following the discussion and developments on these subjects we refer to [65].

5.5 Conclusion

In this section we have followed the work on improving the convergence properties of the Gutzwiller-Voros zeta function by introducing new evolution operators that yield a larger domain of analyticity and at the same time still gives the correct semiclassical resonances. First we studied the "quantum Fredholm" determinant which was (historically) our first candidate for this. This determinant has convergence properties that are superior to the Gutzwiller-Voros zeta function, but unfortunately it does not give the correct nonleading resonances. Next we followed the work of Vattay and studied an evolution operator which is multiplicative and therefore gives an entire spectral determinant. We derived the general N-dimensional expression for this determinant in terms of the cycle stabilities, and made a few numerical 3-disk investigations on our result. In contrast to the Gutzwiller-Voros zeta function which is only an asymptotic series, the Vattay determinant converges to the right resonances by inclusion of still more and more orbits. It has however, certain disadvantages as well: first, to get the quantum resonances with large negative imaginary part one has to include many more periodic orbits in the calculation of the determinant than in the Gutzwiller-Voros zeta function case. In the Gutzwiller-Voros zeta function case on the other hand, inclusion of longer orbits makes the determinant diverge and destroys all the previously obtained lowlying resonances. Second, the Vattay determinant has resonances that are not at all related to the physical

problem, - a problem which one does not encounter in the Gutzwiller-Voros zeta function. One can hope that it will be possible to filter out these fake resonances by the technique used in [14].